

Resonant enhancement of second order sideband generation for intraexcitonic transitions in GaAs/AlGaAs multiple quantum wells

M. Wagner,^{1,a)} H. Schneider,¹ S. Winnerl,¹ M. Helm,¹ T. Roch,² A. M. Andrews,² S. Schartner,² and G. Strasser²

¹Institute of Ion Beam Physics and Materials Research, Forschungszentrum Dresden-Rossendorf, P.O. Box 510119, 01314 Dresden, Germany

²Micro- and Nanostructure Center (ZMNS), TU Wien, Floragasse 7, 1040 Vienna, Austria

(Received 5 May 2009; accepted 26 May 2009; published online 16 June 2009)

We present an experimental study on efficient second order sideband generation in symmetric undoped GaAs/AlGaAs multiple quantum wells. A near-infrared laser tuned to excitonic interband transitions is mixed with an in-plane polarized terahertz beam from a free-electron laser. The terahertz beam is tuned either to the intraexcitonic heavy-hole $1s$ - $2p$ transition or to the interexcitonic heavy-hole light-hole transition. We find strong evidence that the intraexcitonic transition is of paramount influence on $n = \pm 2$ sideband generation, leading to an order-of-magnitude resonant enhancement of the conversion efficiency up to 0.1% at low temperature. At room temperature, the efficiency drops only by a factor of 7 for low terahertz powers. © 2009 American Institute of Physics. [DOI: 10.1063/1.3155189]

Strong ac fields in the terahertz (THz) region are known to modify interband absorption of semiconductor heterostructures. Besides shifts of the excitonic energies, for instance due to the ac-Stark effect¹ or dynamical Franz-Keldysh effect,² strong THz fields can lead to spectral sidebands of an interband excitation. Sidebands have been studied in bulk GaAs,³ but especially in semiconductor heterostructures using magnetoexcitons and excitonic and electronic intersubband transitions.^{4–8} Besides high conversion efficiencies, semiconductor heterostructures have the advantage that intersubband energies can be tuned by applying a dc field,⁹ making these devices potentially attractive for electrically controlled switches and modulators.

In THz sideband generation, the ac THz field with a frequency ω_{THz} modulates the polarization induced by a near-infrared (NIR) beam of frequency ω_{NIR} . New frequencies result at $\omega = \omega_{\text{NIR}} \pm n\omega_{\text{THz}}$. In symmetric structures, n is restricted to even integer numbers,⁴ whereas in asymmetric quantum wells also odd sidebands are allowed.¹⁰ Sideband generation at weak THz fields can be modeled using a nonlinear susceptibility and low-order perturbation theory.^{10,11} Highest reported efficiencies in quantum wells for an $n = +1$ process were around 0.2% in a THz waveguide geometry with the THz beam tuned to an excitonic hole intersubband transition.¹² For $n = +2$, slightly lower efficiencies were reported for magnetoexcitons in strong magnetic fields.⁵

Here, we report on efficient $n = \pm 2$ sideband generation up to room temperature in a relatively simple geometry. We employ an in-plane THz field in an effective three-level system, consisting of the $1s$ and $2p$ states of the heavy-hole (hh) exciton, and the $1s$ state of the light-hole (lh) exciton in multiple quantum wells (MQWs). Note that no magnetic field is needed to separate the energy levels. We demonstrate experimentally how the $n = \pm 2$ sideband efficiency scales when the THz beam is tuned between interexcitonic hh-lh and intraexcitonic hh($1s$ - $2p$) transitions.

The experimental scheme is indicated in Fig. 1(a). A tunable NIR Ti:sapphire laser delivering 2.5 ps long pulses is transmitted through the sample and detected by a charge coupled device camera attached to a grating spectrometer. The sample studied consists of 60 periods of undoped GaAs quantum wells, each 8.2-nm-thick and separated by 19.6-nm-thick barriers of $\text{Al}_{0.34}\text{Ga}_{0.66}\text{As}$. To allow transmission measurements, the sample was glued to NIR-transparent (100)-oriented ZnTe and the semi-insulating GaAs substrate has been etched away. The sample was kept in a liquid He flow cryostat equipped with a diamond window for the strong THz beam which is overlapped with the NIR beam near normal incidence on the sample. We employ FELBE, the free-electron laser (FEL) at the Forschungszentrum Dresden-

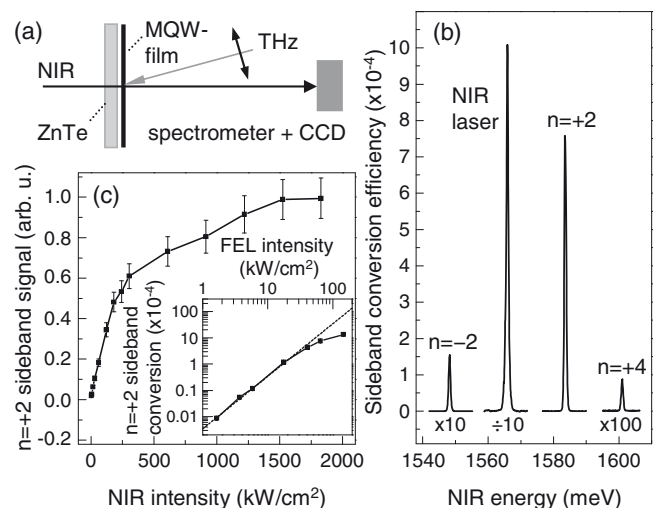


FIG. 1. (a) Experimental setup. (b) Transmitted sideband spectrum at 10 K for $\hbar\omega_{\text{THz}} = 8.9$ meV near the hh($1s$ - $2p$) transition. For clarity, the $n = -2$ and $n = +4$ sidebands are multiplied by 10 and 100, respectively, and the NIR laser is divided by 10. The THz peak intensity was around 65 kW/cm^2 . The NIR intensity was 3 kW/cm^2 . (c) For an FEL peak intensity of about 8 kW/cm^2 the $n = +2$ sideband signal depends linearly on NIR intensity until saturation is reached. The inset shows the quadratic behavior of the $n = +2$ sideband with FEL intensity (the dotted line is a quadratic fit).

^{a)}Electronic mail: m.wagner@fzd.de.

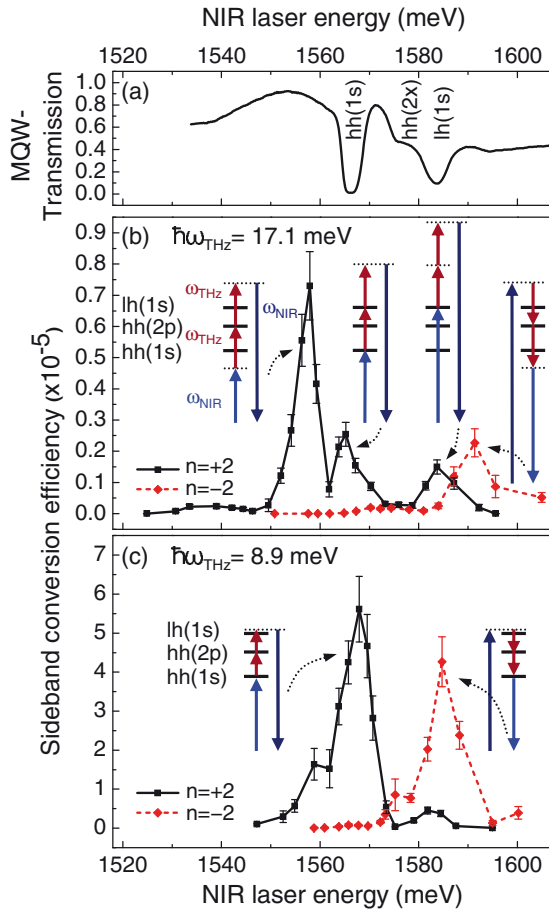


FIG. 2. (Color online) (a) MQW film transmission spectrum at 10 K with hh(1s), hh(2x), and lh(1s) transition (x marks the s and p state). (b) Sideband spectra for $n=+2$ (black line) and $n=-2$ (red dashed line) for an NIR intensity of 180 kW/cm², an FEL intensity around 18 kW/cm² and an FEL energy of 17.1 meV, corresponding to the hh(1s)-lh(1s) transition. Schematic level diagrams indicate the involved transitions. (c) Same as (b) for an FEL energy of 8.9 meV near the estimated hh(1s-2p) resonance.

Rosendorf. This THz source can be tuned continuously from 6 to 300 meV and delivers pulses at a repetition rate of 13 MHz with pulse durations of 10–25 ps for the energies used here. The NIR laser repetition rate was also reduced down to 13 MHz by an acousto-optical pulse picker to temporally overlap each NIR pulse with an FEL pulse. The polarizations of the FEL and NIR laser were linear and parallel to each other for maximum sideband signal.

Figure 2(a) shows the transmission spectrum of the thin MQW film, obtained through normalizing the signal by the ZnTe substrate transmission. hh and lh exciton transitions can be distinguished. At an energy of 1575 meV, the onset of the hh continuum transitions can be seen, starting with the interband allowed hh(2s) exciton state. The nearby 2p state is optically interband forbidden but should lie around 9 meV above the hh(1s) transition.¹³ However, the excitonic inter-subband transition between hh(1s) and hh(2p) exciton states is allowed and couples strongly to THz radiation.^{2,5}

In Fig. 1(b), a typical low-temperature sideband spectrum is measured under FEL illumination with the NIR laser tuned near the hh(1s) exciton energy. Different even orders of sidebands could be observed. Due to slight asymmetry of the quantum wells resulting from MBE growth, also the odd sidebands $n = \pm 1$ appear with typical intensities 1000 times smaller than $n = \pm 2$ (not shown here). Corrected for the

losses in the ZnTe substrate, the $n=+2$ sideband reveals a conversion efficiency between incoming NIR power and emitted sideband of 0.13% for an FEL intensity of 145 kW/cm², which is high for an $n=+2$ process.¹²

In Fig. 1(c), the $n=+2$ sideband power with the NIR laser at the hh(1s) resonance depends linearly on the NIR intensity until saturation is reached. The following experiments were performed at an NIR peak intensity of 180 kW/cm² on the quantum well film, resulting in an exciton density at the strongly absorbing hh(1s) exciton of 3×10^{10} cm⁻². A measurement with 10% of this relatively high exciton density was also taken but the trends presented here stayed the same and only a reduced linewidth was observed. The inset of Fig. 1(c) displays the quadratic dependence of the $n=+2$ power with FEL intensity, as expected for this $\chi^{(3)}$ process.

Now, in Fig. 2(b), the NIR laser energy was tuned at a fixed FEL energy, and at each position, the $n=+2$ (black line) and $n=-2$ (red dashed line) sideband power was recorded. First, we address the case where the FEL energy is fixed at 17.1 meV, corresponding to the interexcitonic hh(1s)-lh(1s) separation. For the $n=+2$ sideband, three pronounced resonances are observed and their origin can be seen qualitatively from the schematic energy level diagrams. The strongest resonance at 1557 meV lies slightly below the band edge. One FEL-photon energy above we find the hh(2s) and hh(2p) state in the transmission spectrum, serving as an intermediate state for the mixing. The relative strength of the resonance peak shows that the 1s-2p transition couples strongly to the THz radiation, although the NIR laser is only resonant with a virtual level and the final state lies in the continuum above the lh. The sideband resonance signal at the hh(1s) state is smaller, although one FEL photon is resonant with the hh(1s)-lh(1s) transition. However, for small in-plane wave vectors, this transition is weak.¹⁴ The third resonance at the lh(1s) position is less pronounced since the lh exciton is coupled to continuum states and not to sharper excitonic states like in the aforementioned cases. Note that the intraband optically allowed hh(2s) state does not lead to a pronounced feature in the sideband resonance scan. The $n=-2$ sideband spectrum is consistent with this picture, showing highest conversion signal when the NIR laser is tuned 17.1 meV above the hh(2p) state. Thus we find that the hh(2p) state as an intermediate state for the nonlinear mixing dominates both the $n=+2$ and $n=-2$ sideband spectra.

We now address the case where the FEL energy is fixed at 8.9 meV near the estimated hh(1s-2p) resonance. The corresponding NIR sideband spectrum is shown in Fig. 2(c). One observes an increase in the $n=+2$ sideband signal at the hh exciton by a factor of 20. Now the FEL is resonant with the hh(1s-2p) transition and also approximately with the hh(2p)-lh(1s) transition, leading to an efficient $n=-2$ generation as well. The $n=+2$ spectrum shows a weak resonance at 1583 meV at the lh(1s) state, similar to Fig. 2(b). The additional small shoulders at 1575 meV (for $n=-2$) and 1559 meV (for $n=+2$) cannot be assigned with absolute certainty to a particular resonance.¹⁵

At a temperature of 77 K, there is no drop in efficiency compared to the low-temperature measurement. At room temperature, the $n=+2$ sideband resonance broadens, as shown in Fig. 3, for a THz intensity of 18 kW/cm² (black line) and 41 kW/cm² (red dashed line). The broadening

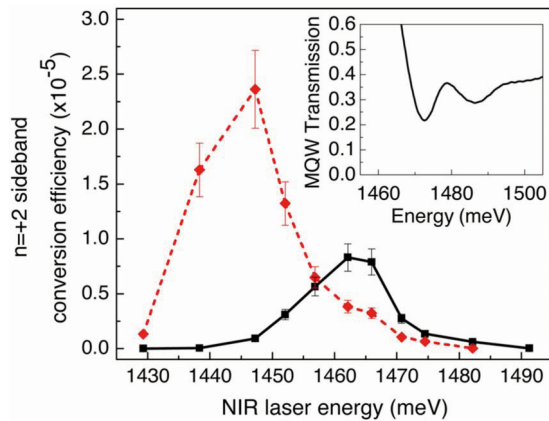


FIG. 3. (Color online) $n=+2$ sideband resonance taken above room temperature for an NIR intensity of 180 kW/cm^2 , an FEL intensity of 18 kW/cm^2 (black line) and 41 kW/cm^2 (red dashed line). The FEL energy is fixed at 8.9 meV . Due to pronounced lattice heating, the sideband spectra appear shifted to lower energies by around 7 meV (black line) and 24 meV (red dashed line), respectively, with respect to the MQW transmission without FEL (inset, taken at 290 K).

stems from broader excitonic resonances in the transmission spectrum (Fig. 3 inset). Nevertheless, at lower THz intensities of 18 kW/cm^2 , we still find an efficiency which is only reduced by a factor of 7 compared to the 10 K measurement. The FEL energy was kept at 8.9 meV , though the hh-lh splitting decreases from 17 to 14 meV . However, with the broader absorption lines, the need for matching the THz energy exactly with the energy levels is relaxed. Note that both spectra differ in the spectral position from the transmission measurement taken at 290 K . To overlap them with the transmission measurement, they have to be shifted to higher energies by 7 and 24 meV , respectively. This shift in bandgap is due to a pronounced FEL-induced lattice heating by roughly 17 and 52 K for 18 and 41 kW/cm^2 , respectively.

In summary, we have demonstrated efficient $n = \pm 2$ sideband generation in a GaAs/AlGaAs MQW film with the THz beam under normal incidence. Relatively high conversion efficiencies of the $1.7 \mu\text{m}$ thin quantum well film above 0.1% were measured despite somewhat broad linewidths. By tuning the THz energy in resonance with the hh($1s-2p$) tran-

sition, we showed that this intraexcitonic transition dominates the sideband spectra compared to a THz energy of the interexcitonic transition between hh and lh states. Slightly above room temperature, the sideband efficiency drops only by a factor of 7. Together with the possibility of shifting the sample's exciton transitions via an applied bias,⁹ one could think of efficient room temperature switches or modulators based on such systems.

We gratefully acknowledge discussions with D. Citrin, J. Kono, and D. Stehr. We thank P. Michel and his ELBE team, as well as W. Seidel for their dedicated support. The Vienna group is supported by the Austrian FWF.

- ¹J. F. Dynes, M. D. Frogley, M. Beck, J. Faist, and C. C. Phillips, *Phys. Rev. Lett.* **94**, 157403 (2005).
- ²K. B. Nordstrom, K. Johnsen, S. J. Allen, A.-P. Jauho, B. Bimir, J. Kono, T. Noda, H. Akiyama, and H. Sakaki, *Phys. Rev. Lett.* **81**, 457 (1998).
- ³M. A. Zudov, J. Kono, A. P. Mitchell, and A. H. Chin, *Phys. Rev. B* **64**, 121204 (2001).
- ⁴J. Černe, J. Kono, T. Inoshita, M. Sherwin, M. Sundaram, and A. C. Gossard, *Appl. Phys. Lett.* **70**, 3543 (1997).
- ⁵J. Kono, M. Y. Su, T. Inoshita, T. Noda, M. S. Sherwin, S. J. Allen, and H. Sakaki, *Phys. Rev. Lett.* **79**, 1758 (1997).
- ⁶A. V. Maslov and D. S. Citrin, *Phys. Rev. B* **62**, 16686 (2000).
- ⁷V. Ciulin, S. G. Carter, M. S. Sherwin, A. Huntington, and L. A. Coldren, *Phys. Rev. B* **70**, 115312 (2004).
- ⁸S. G. Carter, V. Ciulin, M. Hanson, A. S. Huntington, C. S. Wang, A. C. Gossard, L. A. Coldren, and M. S. Sherwin, *Phys. Rev. B* **72**, 155309 (2005).
- ⁹M. Y. Su, S. G. Carter, M. S. Sherwin, A. Huntington, and L. A. Coldren, *Appl. Phys. Lett.* **81**, 1564 (2002).
- ¹⁰M. Y. Su, C. Phillips, J. Ko, L. Coldren, and M. S. Sherwin, *Physica B* **272**, 438 (1999).
- ¹¹T. Inoshita, J. Kono, and H. Sakaki, *Phys. Rev. B* **57**, 4604 (1998).
- ¹²S. G. Carter, V. Ciulin, M. S. Sherwin, M. Hanson, A. Huntington, L. A. Coldren, and A. C. Gossard, *Appl. Phys. Lett.* **84**, 840 (2004).
- ¹³I. Galbraith, R. Chari, S. Pellegrini, P. J. Phillips, C. J. Dent, A. F. G. van der Meer, D. G. Clarke, A. K. Kar, G. S. Buller, C. R. Pidgeon, B. N. Murdin, J. Allam, and G. Strasser, *Phys. Rev. B* **71**, 073302 (2005).
- ¹⁴F. Szmulowicz and G. J. Brown, *Phys. Rev. B* **51**, 13203 (1995).
- ¹⁵Such a mixing process would include normally forbidden hh($1s-2s$) transitions, which could be possible by assuming a state consisting of mixed hh($2s$) and hh($2p$) contributions and thus relaxing the selection rules. Alternatively, the $n=+2$ shoulder (at 1559 meV) might be induced by an Autler-Townes splitting, see S. G. Carter, V. Birkedal, C. S. Wang, L. A. Coldren, A. V. Maslov, D. S. Citrin, and M. S. Sherwin, *Science* **310**, 651 (2005).